Available online at www.sciencedirect.com

SciVerse ScienceDirect

Ceramics International 38 (2012) 3529–3535

CERAMICS INTERNATIONAL

www.elsevier.com/locate/ceramint

Tunable TiO_2 (anatase and rutile) materials manufactured by mechanical means

Amal K.P.D. Savio [a], David Starikov [b,c], Abdelhak Bensaoula [b], Rajeev Pillai [b], Luis L. de la Torre García [d], Francisco C. Robles Hernández [a,*]

[a] University of Houston, Department of Mechanical Engineering Technology, College of Technology, 304 Technology Building, Houston, TX 77204-4020, United States

[b] University of Houston, Department of Physics, College of Natural Sciences and Mathematics, 733 Science and Research Building 1, Houston, TX 77204-5005, United States

[c] Integrated Micro Sensors, Inc. (IMS), 10814 Atwell Drive, Houston, TX 77096, United States

[d] University of Houston, Texas Manufacturing Assistance Center, College of Technology, 821 TMAC Building, Houston, TX 77204-6023, United States

Received 22 November 2011; received in revised form 22 December 2011; accepted 23 December 2011
Available online 2 January 2012

Abstract

Anatase and rutile are two naturally found titanium dioxide phases with attractive dielectric, catalytic, and photo-catalytic characteristics. Anatase and rutile are photo-catalytically active in the UV region, since their band gaps are 3.2 eV and 3.75 eV, respectively. In this work is proposed a cost-effective, easy to launch methodology for modification of the TiO_2 bandgap. Such modifications will make the oxides photo-catalytically active in a wider optical range from the visible wavelengths to an extended UV spectrum. The proposed methodology is based on mechanical means such as mixing and milling. Various ratios of anatase:rutile were investigated and milled from 0 (mixing only) to 50 h using high energy mills. The results on mixing and milling show that it is possible to modify the bandgap of the TiO_2 from 2.53 eV to 4.04 eV. The characterization was conducted by means of X-ray diffraction, Raman spectroscopy, Scanning electron microscopy, and optical spectroscopy. Published by Elsevier Ltd and Techna Group S.r.l.

Keywords: Bandgap; Titanium dioxide; Spectroscopy; Mechanical milling

1. Introduction

The following are the crystalline structures and symmetries of commonly occurring titanium dioxide (TiO_2) allotropes that are found in nature. Rutile has a $P4_2/mnm$ symmetry and a tetragonal crystalline structure; anatase is $I4_1/amd$ and has a body centered tetragonal and brookite is P/cab with an orthorhombic structure. While rutile is a naturally occurring phase, it can also be obtained from heat treated anatase [1,2]. Anatase seems to be more attractive than rutile for a wide range of applications including: photo catalysis, solar energy conversion, protective surface coating, ceramics, pigments, biological field, food industry, catalysis, as a reductor, photo-corrosion, among others [3–10]. The transformation anatase–rutile is highly dependent on the synthesis (temperature, grain size) and other conditions, such as: purity of the components, specific surface area, porosity, etc. [11–15]. Annealing affects the titanium dioxide microstructure, crystalline structure, phase(s), and grain size, and also the catalytic and photo catalytic efficiencies [16–18]. Previous research had demonstrated that highly pure and nanostructured anatase can be synthesized by sonochemistry [19,20].

The electronic industry can benefit from tunable TiO_2 materials due to its advanced semi-conducting and dielectric properties. Undoped TiO_2 has a high dielectric constant, while it behaves as a wide bandgap semi-conductor when doped. Doped TiO_2 has a high potential for photovoltaic, photo-detector, and chemical sensor applications. On the other hand, undoped anatase is a good dielectric, which has a number of applications in electronics (e.g. capacitors, mos devices, field effect transistors), optical and protection coatings, among other uses. Sonochemically synthesized and doped TiO_2 can reach bandgaps between 2.7 eV and 4.1 eV [21] making it a desirable

* Corresponding author: Mailing address: University of Houston, College of Engineering Technology, 304 Technology Building, Houston, TX 77204-4020, United States. Tel.: +1 713 743 8231; fax: +1 505 213 7106.
E-mail addresses: fcrobles@uh.edu, fcrobles@central.uh.ed (F.C. Robles Hernández).

0272-8842/$36.00. Published by Elsevier Ltd and Techna Group S.r.l.
doi:10.1016/j.ceramint.2011.12.067

tunable oxide that opens opportunities for a variety of applications.

Mechanical milling is a method originally proposed by Gilman and Benjamin in the 60s [22,23]. This method has proven to be successful to manufacture nanostructured materials at room temperature [24–26]. A further advantage of mechanical milling is its potential to sponsor or to hinder in situ reactions or phase transformations by controlling time, atmosphere, media, and temperature [25]. Mechanical milling is an ideal method for producing nanostructured and highly homogeneous powders with desirable grain and particle size for a variety of compositions.

In this paper is presented a new methodology to produce tunable undoped TiO_2 by mechanical means. This cost-effective methodology will have a potential impact on research, science, and industrial applications; in particular for catalytic and photo-catalytic uses in the visible and UV spectral range. The effects of mixing and milling parameters on the optical bandgap of TiO_2 have been investigated in this work. The commercial and mechanically processed TiO_2 powders were characterized using X-ray diffraction (XRD), scanning electron microscopy (SEM), optical spectroscopy (OS), and Raman spectroscopy (RS), and the results are discussed accordingly.

2. Materials and methods

The anatase material used in this work has the following characteristics: 99.7 wt% purity, −325 mesh, surface area (BET) 200–220 m^2/g. Rutile material has the following characteristics: 99.9% purity, particle size <5 μm. Both powders were obtained from Sigma Aldrich. Mechanical milling was conducted on a Spex 8000 M mill for times varying from 0 to 50 h; although, at 0 h of milling the samples were mixed without milling media. The following (anatase:rutile) relative weight ratio systems were investigated: 1:0, 3:1, 1:1, 1:3, and 0:1. No control agent was used during the milling. In order to assure homogeneity in the 3:1, 1:1, and 1:3 systems, the powders were mixed for 10 min in batches of 10 g in acrylic vials without milling media. The commercial (1:0 and 0:1 systems) products were used as purchased.

2.1. Characterization methods

The XRD characterization was conducted on a SIEMENS Diffractometer D5000 equipped with a Cu tube and operated at 40 kV and 30 A with a corresponding $K_\alpha = 0.15406$ nm. The lattice parameters (“a” and “c”) for anatase and rutile phases were determined using the (1 0 1) and (1 1 0) reflections, respectively. The Scherrer method was used to determine the grain size [27] based on the (1 0 1) reflection. The Scherrer equation is as follows: $D = k\lambda/\beta_{1/2}\cos\theta$ where: D is the average diameter of the calculated particles, “k” is the shape factor of the average crystallite (0.9), λ is the wavelength in Å (0.15405 nm), $\beta_{1/2}$ is half width maximum of the X-ray reflection peak. The Scherrer method was selected due to its higher accuracy (±15%) when compared to other methods, such as, for example, Transmission Electron Microscopy (TEM) [28]. The XRD reflections were determined based on JCPDS cards (International Center of Diffraction Data®).

The weight fractions of anatase (W_A) and rutile (W_R) for the commercial, mixed and milled samples were determined using a modified version of the Spurr–Meyer’s method [21,29]. A modified version of the Spurr–Meyer’s equation has been developed and used by the authors of this paper. The modification is based on using the area under the XRD reflections instead of conventionally used reflection’s intensity. The modified model is more accurate, repeatable, and consistent when compared to the traditional approach [21]. The following are the modified Spurr–Meyer’s equations: $W_A = 1/[1 + 0.8A_A/A_R]$ and $W_R = 1/[1 + 1.26A_R/A_A]$ where A_A and A_R are the peaks areas in counts per second (c.p.s.) for the (1 0 1) and (1 1 0) planes for anatase and rutile, respectively.

The SEM observations were carried out on a FEI XL-30FEG using secondary electrons. The samples were prepared by depositing the powders directly on a graphite tape. Raman spectroscopy was conducted on an XploRA™ apparatus, using a green laser (532 nm) on medium intensity and a shift of 1 cm^{-1}, a spot size is 1 μm and a specific resolution of 0.5 cm^{-1}. Optical spectroscopy characterization was conducted using a Triax 320 monochromator equipped with a broad spectrum Xenon lamp and a UV-enhanced Si photodetector. The spectral measurements for powders were performed using the diffused reflectance method in a wavelength range between 250 and 500 nm. The bandgap of the materials was determined with the Kulbeka–Munk method [30].

The samples for Raman and optical spectroscopies were prepared by adding 0.01 g of the respective powders into deionized water. The mix was subjected to sonication for 10 min in a Misonix sonicator S4000 apparatus using a micro-tip, with amplitude of 100% and a frequency of 20 kHz. The sonicator was programmed to shut down if a temperature of 320 K is reached. The suspension was deposited in fuse silica glasses 4 mm in diameter using a spinning-like approach to form TiO_2 films on the fused silica glasses. After the layer is formed, the glasses with the powders were dried on a hot plate at a temperature of 343 K for 2 h. In order to make the deposited films thicker, the spinning operation was repeated 5 times.

3. Results

Fig. 1 shows the results on XRD, Raman, and SEM characterization of commercial anatase and rutile films. From this figure can be seen that commercial anatase contains rutile and vise versa, commercial rutile contains anatase (Fig. 1a, b) in amounts above traces. The exact amount is confirmed by using the modified Spurr–Meyer’s equations. While these results do not claim that commercial anatase and rutile are not a highly pure TiO_2, they indicate that there are measurable amounts of unintended mixed phases in the commercial products. The calculated amounts of unintended anatase and rutile are 3.1 wt% and 1.2 wt%, respectively. The Raman bands identified in Fig. 1b correlate with those reported in Refs. [31,32]. The morphology of the commercial products

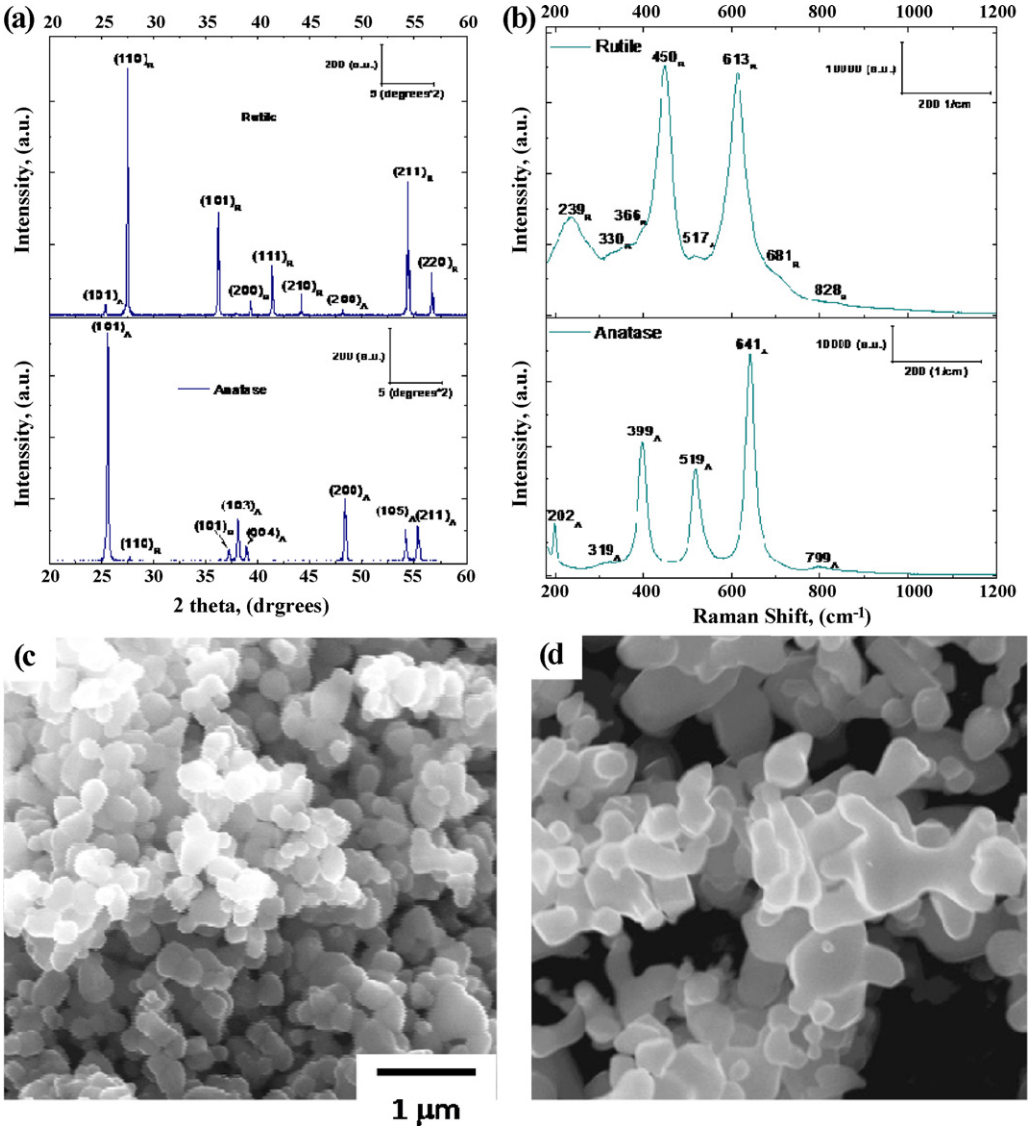

Fig. 1. Characterization of commercial anatase and rutile by means of: (a) X-ray diffraction, (b) Raman spectroscopy and (c, d) scanning electron micrographs of anatase and rutile, respectively. *Note*: the subscripts A and R (a, b) stand for anatase and rutile.

(Fig. 1c and d) is irregular and the average particle size of anatase is smaller than that of rutile particles.

Fig. 2a shows the calculated fractions of anatase/rutile for the investigated TiO_2 systems. From Fig. 2a it is evident that the dynamic change or transformation from anatase to rutile resulted in a decrease of anatase with the increase of the Spex milling time. Similar path is followed for all the investigated systems. This demonstrates that rutile is more stable than anatase [6]. In summary, the reduction of anatase in the commercial sample went from 97 wt% to 66 wt% after 50 h of milling and for the same milling time of the 3:1 system, the amount of anatase decreased from 75 ± 3 wt% to 52 wt%. For 1:1, 1:3, and 0:1 systems Spex milled for 50 h the respective amounts of anatase were: 15 wt%, 6 wt%, and 0.03 wt%.

Fig. 2b shows the change in the grain size for the respective Spex milling times in the investigated TiO_2 systems. From this figure it is clear that grain size decreases as a function of milling time, except for the anatase present in the 0:1 system, where the grain size seems to coarsen from 52 nm to 429 nm. Although, this is an unusual behavior, the phenomenon is attributed to the limited amount of anatase (from 3 wt% to 0.7 wt%) present in the sample that may compromise the accuracy of the method. The grain refining effect during milling is expected due to the nature of milling that consists of a constant breaking and welding of the particles. It is expected that due to the brittleness of TiO_2 the milling process is dominated by fractures with limited welding. The grain sizes of anatase and rutile in the commercial samples are 101.8 ± 9.8 nm and 125.3 ± 16.7 nm, respectively. The smallest grain size of 52.2 nm calculated for anatase was found in the 1:0 system milled for 50 h. The 3:1 system has the rutile with the smallest grain size (42.2 nm) after 50 h of milling.

The calculated lattice parameters and lattice volume for anatase are $a_A = 0.378 \pm 5 \times 10^{-4}$ nm, $c_A = 0.951 \pm 0.03$ nm and $V_A = 0.136 \pm 7 \times 10^{-9}$ nm, respectively. For rutile the lattice characteristics are: $a_R = 0.457 \pm 1 \times 10^{-3}$ nm,

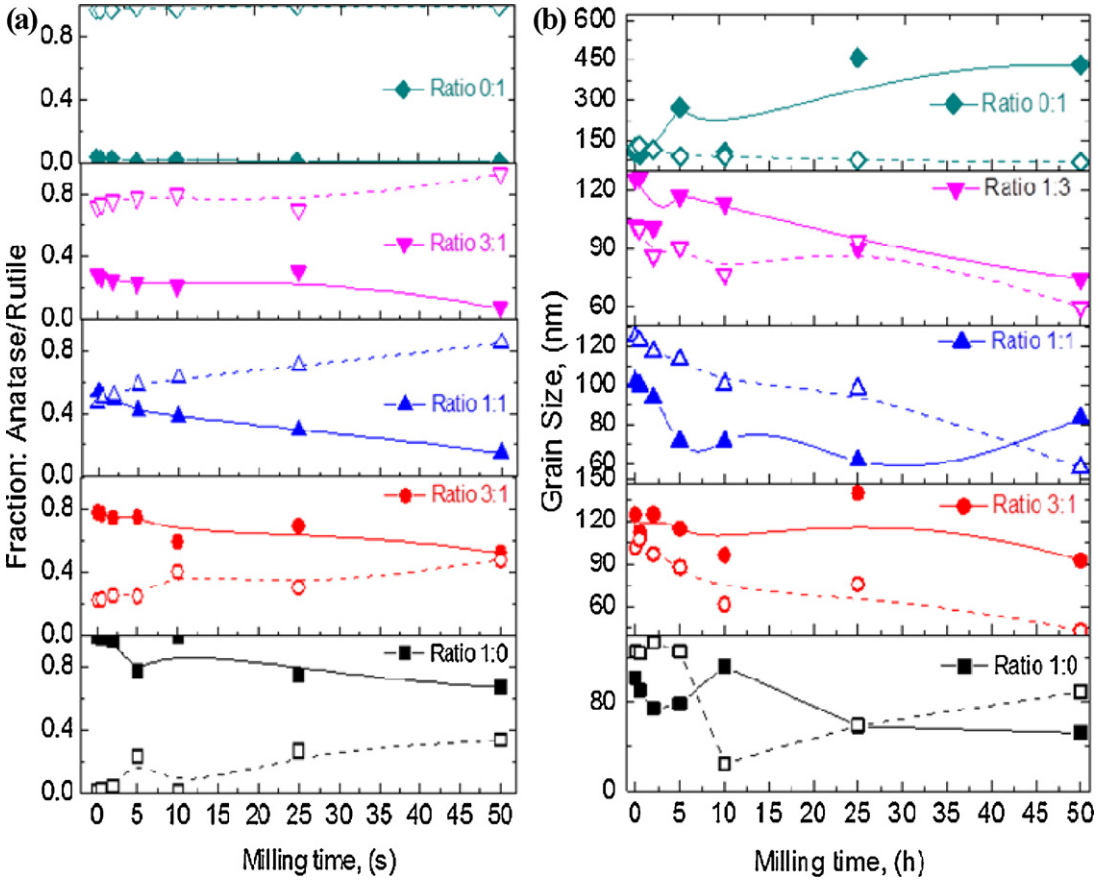

Fig. 2. Dynamic transformation: (a) fraction and (b) grain growth, of anatase and rutile during mechanical milling. The "ratio" indicates the relative fraction anatase:rutile. The solid and empty symbols represent anatase and rutile, respectively.

$c_R = 0.291 \pm 7 \times 10^{-4}$ nm and $V_R = 0.061 \pm 8 \times 10^{-10}$ nm. The average calculated values for the 35 systems have a maximum difference against the theoretical of 0.5% and a standard deviation of 0.03 nm. The residual lattice strain caused by mechanical milling or contamination averages $e_A = 0.54 \pm 27\%$ and $e_R = 0.24 \pm 27\%$ for anatase and rutile, respectively. These results indicate high accuracy and demonstrate that mechanical milling has minimum effects in residual strain. This is expected in ceramics with relatively low fracture toughness that limits their strain capacity.

Fig. 3 is a set of scanning electron micrographs showing the effects of milling on particle morphology. Fig. 3 is an example of the 1:0 system Spex milled from 0 h to 50 h. Similar behavior was observed for the other systems [21]. Commercial anatase (Fig. 3a) is composed of sub-micrometric (~0.3 μm)/semi-spherical particles that are agglomerates of nanostructured grains. These findings were demonstrated by TEM elsewhere [19,20]. After 2 h of milling the powders agglomerate reducing the surface area of the particles and negatively affecting their catalytic potential. On the other hand, the samples milled between 5 and 25 h show particle refinement that is desired in catalysis. After 50 h of milling the particles agglomerate (weld) again, but in this case the agglomerates are denser and smaller than those observed after 2 h of milling (Fig. 3b). The particles observed in Fig. 3 are polycrystalline agglomerates and their grain size determined by the Scherrer method.

Fig. 4 shows the Raman spectrum for the investigated systems after 50 h of Spex milling. The Raman spectrum for both commercial samples, anatase (1:0) and rutile (0:1), show higher intensity than that of the mixed systems (3:1, 1:1, and 1:3). The reduction in the intensity of the Raman peaks for the 3:1, 1:1, and 1:3 systems is attributed to the combined effects characteristic to mixes of commercial powders with various morphology and sizes. The grain size reduction of anatase is attributed to the higher hardness of rutile that resulted in grain refining. The respective hardness values are: 6–6.9 GPa[1] and 8.8–9.6 GPa,[2] for anatase and rutile. Similar trends are observed during grain refining, as shown in Fig. 2.

The intensity of the Raman spectra shown in Fig. 4b was normalized to analyze the relative intensity change for each sample. From this figure it is evident that the B_{1g} (249 cm^{-1}) E_{2g} (440 cm^{-1}) and A_{1g} (610 cm^{-1}) bands for rutile are the most intense along with the E_{2g} (323 cm^{-1}), B_{1g} (359 cm^{-1}) and A_{1g} (534 cm^{-1}) bands for anatase. The anatase Spex milled for 50 h shows that the characteristic Raman bands are evident

[1] http://www.mindat.org/min-213.html as posted on October 06, 2011.
[2] http://www.mindat.org/min-3486.html as posted on October 06, 2011.

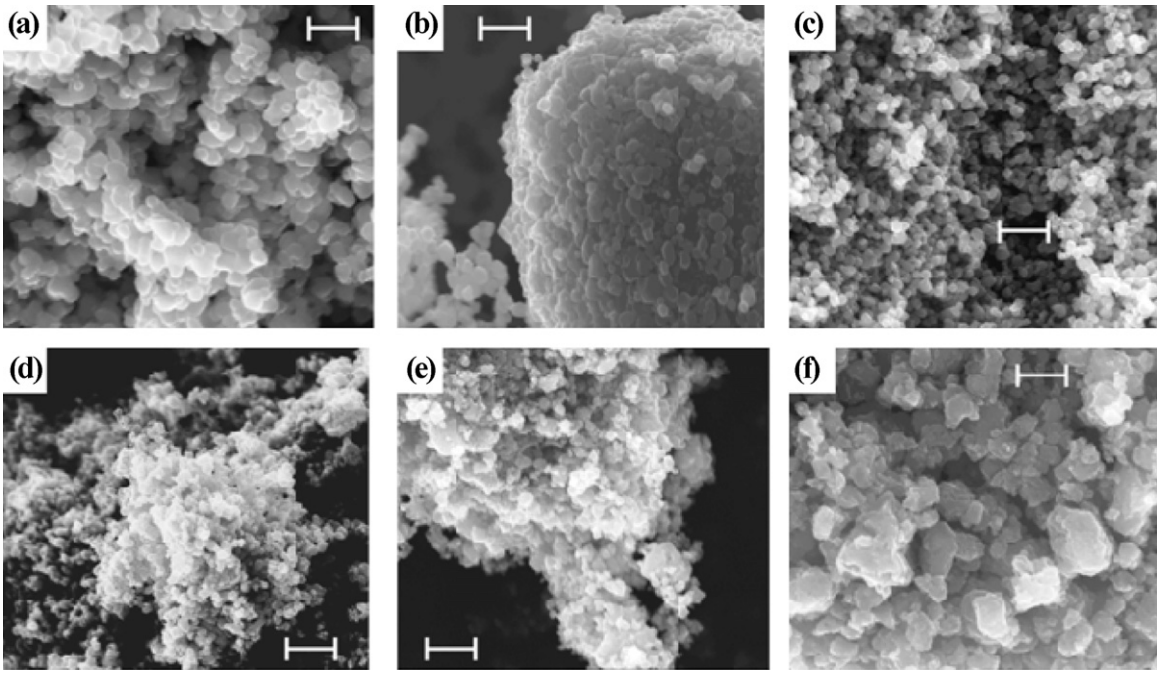

Fig. 3. Dynamic particle evolution of commercial anatase (1:0 system) Spex milled for (a) 0 h, (b) 2 h, (c) 5 h, (d) 10 h, (e) 25 h and (f) 50 h. The scale represents 1 μm.

only in the commercial product, which complicates proper characterization. Therefore, XRD was used as a complementary method (Fig. 4c) allowing a harmonizing characterization of the Spex milled systems. The identification of anatase by XRD is more accurate and allows for determination of the respective fractions of anatase and rutile in the investigated systems.

Fig. 5 shows the dynamic change in the bandgap as a function of the Spex milling time for the investigated TiO_2 systems. It is important to point out that in all cases the bandgap increases as a function of Spex milling time. This behavior is easier to observe at short milling times. In the present work the narrowest band gap of 2.54 eV, was identified for the 1:1 system in the as mixed (0 h milling) conditions, followed by the 2.6 eV commercial anatase (ratio 1:0). On the contrary, the widest band gap (4.06 eV) is observed in commercial rutile (0:1) after 50 h of milling. It is important to note that the band gap in the 0:1 system seems to be unchanged for the first 25 h of milling, but shows a sudden change in the Spex milled sample after 50 h of milling.

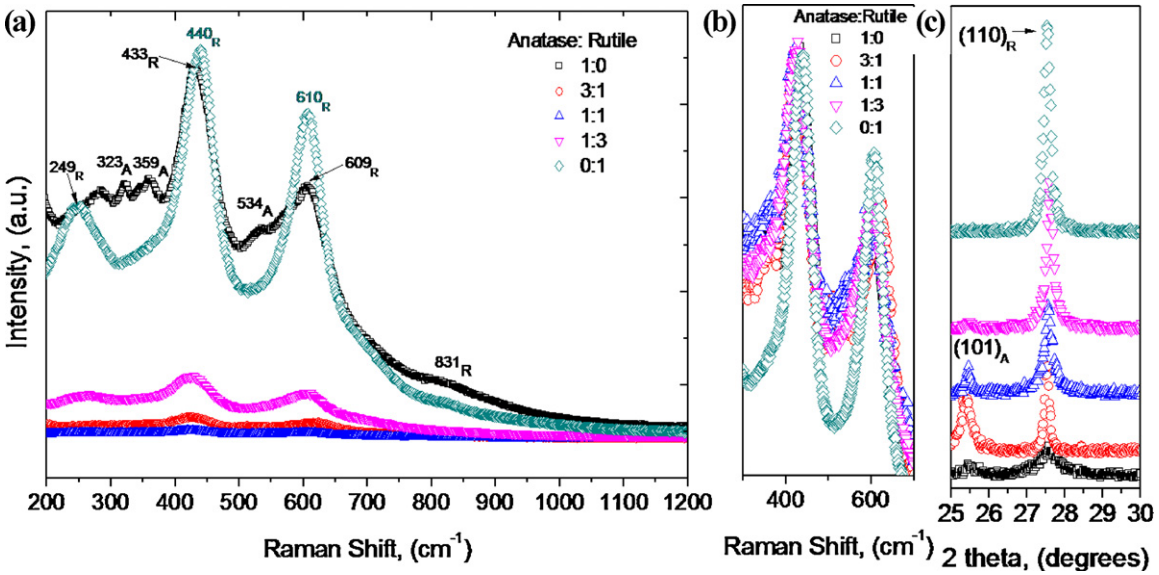

Fig. 4. Characterization of the anatase:rutile systems Spex milled for 50 h by means of Raman (a – relative intensities, b – normalized intensities) and X-ray diffraction (c).

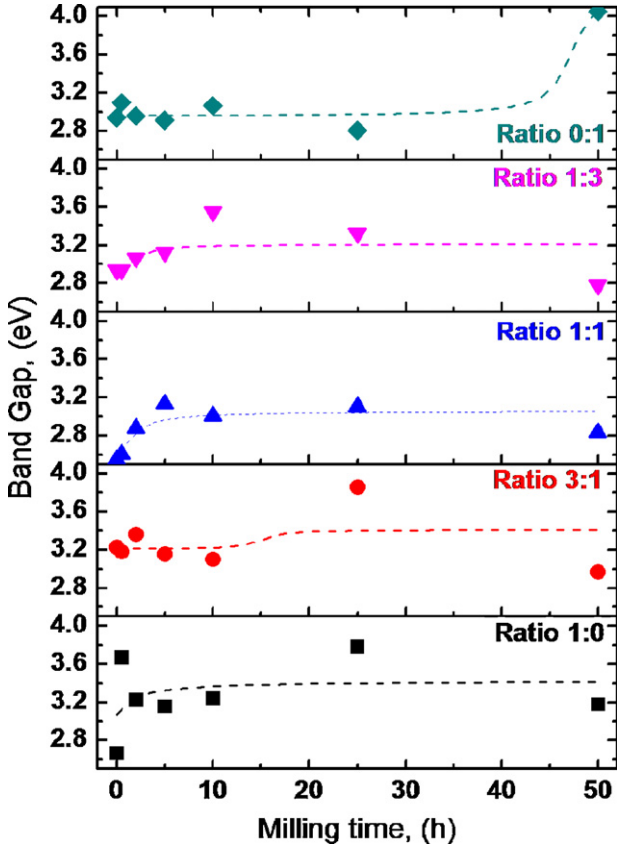

Fig. 5. Bandgap evolution for the investigated TiO_2 samples Spex milled for up to 50 h. The ratio indicates the relative amounts of anatase and rutile.

It follows from Fig. 5 that the investigated samples exhibit a large variation of bandgaps, depending on the system, as well as milling time. However the bandgaps of the commercial products used herein are unusual: 2.6 eV and 2.94 eV for anatase and rutile, respectively. The typical bandgap for pure anatase is 3.2 eV [33] and for pure rutile is 3.7 eV [34]. The band gap values of the samples investigated herein are lower and wider than those presented in combined titanias with other oxides such as SiO_2 [35]. These differences result from measurable amounts of mixed TiO_2 phases in the commercial product. Such reduction of the anatase bangap in the presence of rutile has been previously reported [33]. In addition, the commercial rutile reflects a change in the bangap approaching its standard value, when it reaches higher level of purity (50 h of milling). The same effect cannot be observed in the commercial anatase because it transforms to rutile during Spex milling (Fig. 2a). For comparison purposes and to ensure the accuracy of our results, highly pure anatase was tested and presented a band gap of 3.17 eV confirming the accuracy of our results. The highly pure anatase was synthesized by sonochemistry [21].

4. Discussion

The proposed methodology is effective and has outstanding advantages, since it consists of simple mixing/milling operations that are relatively easy to launch and implement at either research or industrial levels. These simple methods are responsible for quantifiable bandgap effects on anatase:rutile systems allowing the manufacturing of tunable TiO_2 with high potential for catalytic, photo-catalytic, and electronic applications. Additionally, the investigated powders are quite effective for thin film development by methods, such as spinning. The films obtained by this method can be characterized by means of Raman and optical spectroscopy [21]. Potentially the tunable TiO_2 produced herein can be used for tandem type electronic devices that are photo-catalytically active in the visible (blue) and UV regions of the electromagnetic spectrum in the range from 490 nm to 305 nm, respectively.

Two mechanisms that affect the bandgap of TiO_2 were found in the investigated material systems. The first mechanism is the grain size and the second is the fractions of anatase in rutile and rutile in anatase. For instance, in commercial rutile (Fig. 5) the most important parameter affecting the bandgap is the presence of anatase. When the amount of anatase in such system is below 0.3 wt% (50 h of milling) the bandgap changes considerably. From the above-mentioned effects, it is evident that the presence of secondary phases has the strongest impact on the material bandgap.

5. Conclusions

Tunable TiO_2 with bandgap values between 2.54 eV and 4.06 eV can be produced by mechanical means. Such tuning makes the TiO_2 photo-catalytically active in the visible (blue) and UV bands of the optical spectrum. Tunable TiO_2 can be manufactured by mechanical means using commercial products. The main effects that influence the bandgap in TiO_2 are the grain size and the fractions of anatase in rutile and rutile in anatase, the later one having the strongest effect on the bandgap. In fact, relatively small amounts (>0.3 wt%) of rutile in anatase have noticeable effects on bandgap.

Acknowledgements

The authors would like to thank the University of Houston and the State of Texas for their invaluable support through the Star Up, Small grant and HEAFS funding.

References

[1] P.I. Gouma, M.J. Mills, Anatase-to-rutile transformation in titania powders, J. Am. Ceram. Soc. 84 (2001) 619–622.
[2] V.E. Henrich, P.A. Cox, The Surface Science of Metal Oxides, Cambridge University Press, Cambridge, New York, 1994.
[3] N.I. Al-Salim, S.A. Bagshaw, A. Bittar, T. Kemmitt, A.J. McQuillan, A.M. Mills, M.J. Ryan, Characterisation and activity of sol–gel-prepared TiO_2 photocatalysts modified with Ca, Sr or Ba ion additives, J. Mater. Chem. 10 (2000) 2358–2363.
[4] J.H. Braun, Titanium dioxide – a review, J. Coat. Technol. 69 (1997) 59–72.
[5] R.X. Cai, Y. Kubota, T. Shuin, H. Sakai, K. Hashimoto, A. Fujishima, Induction of cytotoxicity by photoexcited TiO_2 particles, Cancer Res. 52 (1992) 2346–2348.
[6] U. Diebold, The surface science of titanium dioxide, Surf. Sci. Rep. 48 (2003) 53–229.
[7] A. Fujishima, X.T. Zhang, Titanium dioxide photocatalysis: present situation and future approaches, CR Chim. 9 (2006) 750–760.

[8] J.Y. Gan, Y.C. Chang, T.B. Wu, Dielectric property of $(TiO_2)(x)$–$(Ta_2O_5)(1-x)$ thin films, Appl. Phys. Lett. 72 (1998) 332–334.
[9] M.R. Hoffmann, S.T. Martin, W.Y. Choi, D.W. Bahnemann, Environmental applications of semiconductor photocatalysis, Chem. Rev. 95 (1995) 69–96.
[10] S. Ito, S. Inoue, H. Kawada, M. Hara, M. Iwasaki, H. Tada, Low-temperature synthesis of nanometer-sized crystalline TiO_2 particles and their photoinduced decomposition of formic acid, J. Colloid Interf. Sci. 216 (1999) 59–64.
[11] A. Burns, G. Hayes, W. Li, J. Hirvonen, J.D. Demaree, S.I. Shah, Neodymium ion dopant effects on the phase transformation in sol–gel derived titania nanostructures, Mater. Sci. Eng. B: Solid 111 (2004) 150–155.
[12] K.N.P. Kumar, K. Keizer, A.J. Burggraaf, T. Okubo, H. Nagamoto, S. Morooka, Densification of nanostructured titania assisted by a phase-transformation, Nature 358 (1992) 48–51.
[13] D.J. Reidy, J.D. Holmes, M.A. Morris, The critical size mechanism for the anatase to rutile transformation in TiO_2 and doped-TiO_2, J. Eur. Ceram. Soc. 26 (2006) 1527–1534.
[14] R.D. Shannon, Phase transformation studies in TiO_2 supporting different defect mechanisms in vacuum-reduced + hydrogen-reduced rutile, J. Appl. Phys. 35 (1964) 3414–3416.
[15] P.A. Smith, R.A. Haber, Reformulation of an aqueous alumina slip based on modification of particle-size distribution and particle packing, J. Am. Ceram. Soc. 75 (1992) 290–294.
[16] C.K. Chan, J.F. Porter, Y.G. Li, W. Guo, C.M. Chan, Effects of calcination on the microstructures and photocatalytic properties of nanosized titanium dioxide powders prepared by vapor hydrolysis, J. Am. Ceram. Soc. 82 (1999) 566–572.
[17] M. Hirano, C. Nakahara, K. Ota, M. Inagaki, Direct formation of zirconia-doped titania with stable anatase-type structure by thermal hydrolysis, J. Am. Ceram. Soc. 85 (2002) 1333–1335.
[18] A.J. Maira, K.L. Yeung, C.Y. Lee, P.L. Yue, C.K. Chan, Size effects in gas-phase photo-oxidation of trichloroethylene using nanometer-sized TiO_2 catalysts, J. Catal. 192 (2000) 185–196.
[19] L. Gonzalez-Reyes, I. Hernandez-Perez, F.C.R. Hernandez, H.D. Rosales, E.M. Arce-Estrada, Sonochemical synthesis of nanostructured anatase and study of the kinetics among phase transformation and coarsening as a function of heat treatment conditions, J. Eur. Ceram. Soc. 28 (2008) 1585–1594.
[20] F.C.R. Hernandez, L. Gonzalez-Reyes, I. Hernandez-Perez, Effect of coarsening of sonochemical synthesized anatase on BET surface characteristics, Chem. Eng. Sci. 66 (2011) 721–728.
[21] P.D.S. Amal Kennedy, Department of Engineering Technology, University of Houston, Houston, TX, 2011, p. 151.
[22] J.S. Benjamin, Mechanical alloying, Powder Metall. Int. 12 (1980) 43.
[23] P.S. Gilman, J.S. Benjamin, Mechanical alloying, Annu. Rev. Mater. Sci. 13 (1983) 279–300.
[24] V. Garibay-Febles, H.A. Calderon, F.C. Robles-Hernadez, M. Umemoto, K. Masuyama, J.G. Cabanas-Moreno, Production and characterization of (Al,Fe)–C (graphite or fullerene) composites prepared by mechanical alloying, Mater. Manuf. Process 15 (2000) 547–567.
[25] J. Guerrero-Paz, F.C. Robles-Hernandez, R. Martinez-Sanchez, D. Hernandez-Silva, D. Jaramillo-Vigueras, Particle size evolution in non-adhered ductile powders during mechanical alloying, Mater. Sci. Forum. 360–3 (2001) 317–322.
[26] F.C. Robles-Hernandez, H.A. Calderon, Nanostructured metal composites reinforced with fullerenes, JOM – US 62 (2010) 63–68.
[27] B.D. Cullity, Elements of X-ray Diffraction, 2nd ed., Addison-Wesley Pub. Co, Reading, Mass, 1978.
[28] E.J. Lavernia, Z. Zhang, F. Zhou, On the analysis of grain size in bulk nanocrystalline materials via X-ray diffraction, Metall. Mater. Trans. A 34A (2003) 1349–1355.
[29] R.A. Spurr, H. Myers, Quantitative analysis of anatase–rutile mixtures with an X-ray diffractometer, Anal. Chem. 29 (1957) 760–762.
[30] M.A. Zanjanchi, H. Noei, M. Moghimi, Rapid determination of aluminum by UV–vis diffuse reflectance spectroscopy with application of suitable adsorbents, Talanta 70 (2006) 933–939.
[31] L. Gonzalez-Reyes, I. Hernandez-Perez, F.C.R. Hernandez, Effect of coarsening of sonochemical synthesized anatase on BET surface characteristics, Chem. Eng. Sci. 66 (2011) 721–728.
[32] V. Swamy, B.C. Muddle, Q. Dai, Size-dependent modifications of the Raman spectrum of rutile TiO_2, Appl. Phys. Lett. 89 (2006) 1631181–1631183.
[33] L. Gonzalez-Reyes, I. Hernandez-Perez, L.D.B. Arceo, H. Dorantes-Rosales, E. Arce-Estrada, R. Suarez-Parra, J.J. Cruz-Rivera, Temperature effects during Ostwald ripening on structural and bandgap properties of TiO_2 nanoparticles prepared by sonochemical synthesis, Mater. Sci. Eng. B: Adv. 175 (2010) 9–13.
[34] D.C. Cronemeyer, Electrical and optical properties of rutile single crystals, Phys. Rev. 87 (1952) 876–886.
[35] D.M. Tobaldi, A. Tucci, A.S. Skapin, L. Esposito, Effects of SiO_2 addition on TiO_2 crystal structure and photocatalytic activity, J. Eur. Ceram. Soc. 30 (2010) 2481–2490.